12. S. E. Haynesworth, M. A. Baber, A. I. Caplan, *Bone* **13**, 69 (1992).
13. M. K. Majumdar *et al.*, *J. Cell. Physiol.* **176**, 57 (1998).
14. S. P. Bruder *et al.*, *Clin. Orthop. Relat. Res.* **355S**, S247 (1998).
15. R. Bucala, L. A. Spiegel, J. Chesney, M. Hogan, A. Cerami, *Mol. Med.* **1**, 71 (1994).
16. These fibroblasts represented middle passage newborn foreskin fibroblasts (Hs27), which were obtained at passage 14 from the American Type Culture Collection (ATCC), and early passage adult skin fibroblasts (1087Sk), which were obtained at passage 1 from ATCC, both with normal karyotype.
17. M. F. Pittenger, U.S. Patent 5, 827, 740 (1998).
18. Murine cDNA probes for LPL and PPARγ2 were the gift of J. Gimble (University of Oklahoma, School of Medicine, Oklahoma City). Polyclonal antibody to aP2 was provided by M. D. Lane (Johns Hopkins University, School of Medicine, Baltimore, MD).
19. A. M. Mackay, S. C. Beck, J. M. Murphy, F. P. Barry, M. F. Pittenger, *Tissue Eng.* **4**, 472 (1998); J. U. Yoo *et al.*, *J. Bone Joint Surg. Am. Vol.* **80A**, 1745 (1998).
20. G. R. Srinivas, H. J. Barrach, C. O. Chichester, *J. Immunol. Methods* **159**, 53 (1994).
21. S. P. Bruder, N. Jaiswal, S. E. Haynesworth, *J. Cell. Biochem.* **64**, 278 (1997); N. Jaiswal, S. E. Haynesworth, A. I. Caplan, S. P. Bruder, *ibid.*, p. 295; S. P. Bruder *et al.*, *J. Bone Miner. Res.* **13**, 655 (1998).
22. We thank D. Fink, J. Andres, R. Deans, F. Barry, S, Bruder, M. Thiede, A. Moseley, and J. Burns for discussion and review of the manuscript; M. Black and M. Earlington for cell isolation from marrow; and D. Sterchi, D. Brown, and J. Skwarek for histology. This work was supported by Osiris Therapeutics (www.osiristx.com) and, in part, by a research contract from the Defense Advanced Research Projects Agency.

22 January 1999; accepted 4 March 1999

Two Distinct Cytokines Released from a Human Aminoacyl-tRNA Synthetase

Keisuke Wakasugi and Paul Schimmel*

Aminoacyl-tRNA synthetases catalyze aminoacylation of transfer RNAs (tRNAs). It is shown that human tyrosyl-tRNA synthetase can be split into two fragments with distinct cytokine activities. The endothelial monocyte–activating polypeptide II–like carboxy-terminal domain has potent leukocyte and monocyte chemotaxis activity and stimulates production of myeloperoxidase, tumor necrosis factor-α, and tissue factor. The catalytic amino-terminal domain binds to the interleukin-8 type A receptor and functions as an interleukin-8–like cytokine. Under apoptotic conditions in cell culture, the full-length enzyme is secreted, and the two cytokine activities can be generated by leukocyte elastase, an extracellular protease. Secretion of this tRNA synthetase may contribute to apoptosis both by arresting translation and producing needed cytokines.

Aminoacyl-tRNA synthetases are ancient proteins that are essential for decoding genetic information in translation. In higher eukaryotes, nine aminoacyl-tRNA synthetases associate with at least three other polypeptides to form a supramolecular multienzyme complex (*1*). Each of these nine eukaryotic tRNA synthetases has an additional domain appended to the NH_2- or COOH-terminal end of the core enzyme, which itself is closely related to the respective prokaryotic counterpart (*2*). In most cases, the appended domains appear to contribute to the assembly of the multienzyme complex (*2*). However, the presence of an extra domain is not strictly correlated with the association of a synthetase into the multienzyme complex. For example, human tyrosyl-tRNA synthetase (TyrRS) has an extra domain at the COOH-terminus compared to prokaryotic and lower eukaryotic TyrRSs (Fig. 1) (*3*), and bovine and rabbit TyrRSs are also suggested to contain an extra domain (*4*). Yet, higher eukaryotic TyrRS is not a component of the multienzyme complex (*1*). Interestingly, the COOH-terminal domain of human TyrRS has 51% sequence identity to the mature form of human endothelial monocyte–activating polypeptide II (EMAP II) (*3*). TyrRS is the only higher eukaryotic aminoacyl-tRNA synthetase known to contain an EMAP II–like domain. In initial experiments, we found that this domain was dispensable for aminoacylation in vitro and in yeast (*5–7*).

EMAP II is a proinflammatory cytokine that was initially identified as a product of murine methylcholanthrene A–induced fibrosarcoma cells (*8*). Pro–EMAP II is cleaved and is secreted from apoptotic cells to produce a biologically active 22-kD mature cytokine (*8, 9*). The mature EMAP II can induce migration of mononuclear phagocytes (MPs) and polymorphonuclear leukocytes (PMNs); it also stimulates the production of tumor necrosis factor-α (TNFα) and tissue factor by MPs and the release of myeloperoxidase from PMNs (*8*).

We investigated each of these five activities with the cloned COOH-terminal domain of human TyrRS and with the full-length enzyme that contains the COOH-terminal domain fused to the catalytic core (*5*). The COOH-terminal domain induced migration of human MPs from peripheral blood (*10*) to an extent comparable to that seen with mature human EMAP II (Fig. 2A). In contrast, no chemotaxis was observed with the full-length TyrRS. The COOH-terminal domain of TyrRS also stimulated TNFα and MP tissue factor activities (Fig. 2, A and B), induced release of PMN myeloperoxidase activity in the peroxidase generation assay (Fig. 2B), and induced PMN migration in chemotaxis chambers (Fig. 2C). The induction of PMN migration by the COOH-terminal domain and mature EMAP II showed the bell-shaped concentration dependence that is characteristic of chemotactic cytokines (*7, 11*). Human full-length TyrRS had none of these properties (Fig. 2, B and C).

We also investigated the NH_2-terminal catalytic domain (mini TyrRS) in the same assays. Human "mini" TyrRS did not induce migration of MPs and did not stimulate TNFα and tissue factor production by MPs (Fig. 2, A and B). Surprisingly, incubation of PMNs with mini TyrRS induced PMN migration (Fig. 2C), and this activity showed a bell-shaped concentration dependence (*7*).

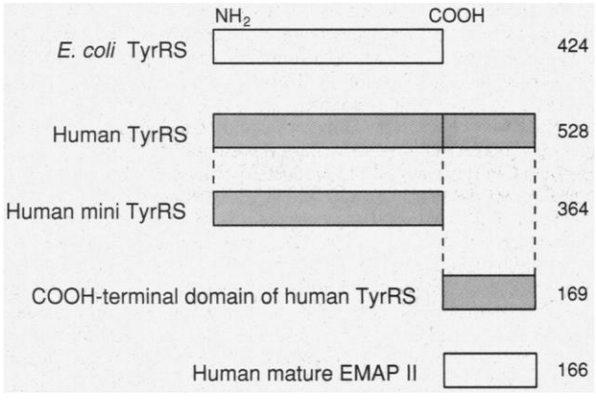

Fig. 1. Schematic representation of the TyrRS constructs used in this study. Alignments of truncated human TyrRSs with human full-length TyrRS (*3, 25*), *E. coli* TyrRS (*26*), and mature human EMAP II (*8*) are depicted schematically. Numbers at right indicate protein size in amino acids.

The Skaggs Institute for Chemical Biology, The Scripps Research Institute, Beckman Center, 10550 North Torrey Pines Road, La Jolla, CA 92037, USA.

*To whom correspondence should be addressed. E-mail: schimmel@scripps.edu

These results raised the possibility that mini TyrRS is a leukocyte chemoattractant. The PMN response to mini TyrRS added to the lower compartment of a chemotaxis chamber was attenuated by addition of mini TyrRS to the upper well (*7*), indicating that enhanced PMN migration was due to chemotaxis, not simply chemokinesis [stimulated random movement (*12*)]. *Escherichia coli* TyrRS, which is similar in size to human mini TyrRS, was inactive in all assays (Fig. 2).

As representative leukocyte chemoattractants, α-chemokines (CXC-chemokines) have a conserved Glu-Leu-Arg (ELR) motif preceding the first cysteine at the NH_2-terminus (*13*). The ELR motif is critical for receptor binding and neutrophil activation (*14*). Human mini TyrRS also has an ELR motif within the catalytic domain that consists of a Rossmann nucleotide-binding fold (Fig. 3A). To investigate the significance of this motif, we prepared a human mini TyrRS mutant in which the ELR motif was mutated to ELQ (Glu-Leu-Gln), because the Arg of this motif is particularly important for receptor binding (*14*). The R → Q mutant mini TyrRS did not induce migration of PMNs (Fig. 2C), suggesting that the ELR motif in mini TyrRS has an important role in PMN receptor binding, as it does in α-chemokines.

To study the interaction of human mini TyrRS with PMNs, we radioiodinated the protein (*15*) for binding studies. Incubation of ^{125}I–mini TyrRS with PMNs led to dose-dependent specific binding at 4°C, which gave linear Scatchard plots (the apparent dissociation constant K_d = 21 nM; 23,000 receptors/PMN). Competitive binding studies (*16*) demonstrated inhibition of binding of ^{125}I–mini TyrRS in the presence of excess amounts of unlabeled mini TyrRS (Fig. 3B). In contrast, human full-length TyrRS, R → Q mini TyrRS, and *E. coli* TyrRS were not competitors (Fig. 3B). Thus, the lack of effect on PMN chemotaxis of full-length TyrRS, R → Q mini TyrRS, and *E. coli* TyrRS is consistent with their lack of binding to PMNs. Finally, neither the COOH-terminal domain of human TyrRS nor mature EMAP II inhibited ^{125}I–mini TyrRS binding to PMNs (Fig. 3B). Thus, the PMN receptor for mini TyrRS is different from that for the COOH-terminal domain or for mature EMAP II.

We next investigated whether α-chemokines with the ELR motif can bind to the same PMN receptor that binds mini TyrRS. We studied interleukin-8 (IL-8), melanoma growth stimulatory activity (Groα), and neutrophil activating protein-2 (NAP-2) (*13*). IL-8 binds to IL-8 receptors type A and type B (also known as CXCR1 and CXCR2, respectively), whereas Groα and NAP-2 bind to the IL-8 receptor type B (*13, 17*). IL-8 inhibited ^{125}I–mini TyrRS binding almost completely, whereas Groα and NAP-2 did not significantly inhibit the binding (Fig. 3B). These results suggest that mini TyrRS specifically binds to the IL-8 receptor type A. To gain further insight into the receptor for mini TyrRS, we studied RBL2H3 rat basophilic leukemia cells that had been transfected with the gene for IL-8 receptor type A or type B (*18*). (Untransfected basophilic leukemia cells express neither receptor.) Mini TyrRS

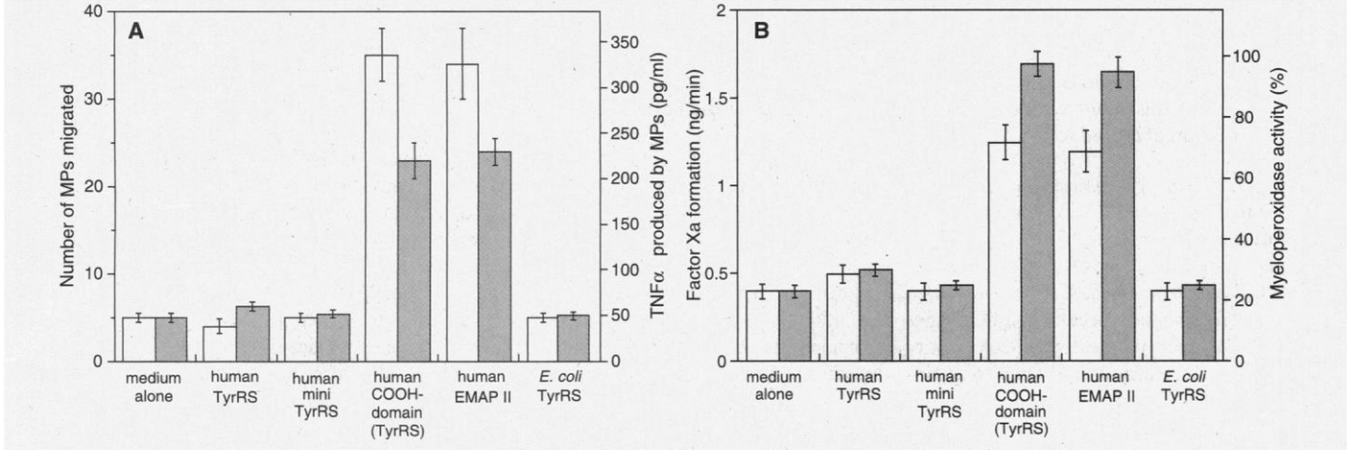

Fig. 2. Effects of several proteins on human MPs and PMNs. (**A**) MP chemotaxis (white bars) and MP production of TNFα (gray bars). The chemotaxis assays were performed in a microchemotaxis chamber ChemoTX (Neuro Probe, Gaithersburg, MD) containing polycarbonate filters (5-μm pores) with polyvinylpyrrolidone (PVP). Each protein (1 nM) or medium alone was added to the lower compartment of chemotaxis chambers, and MPs (10^4 cells) were added to the upper compartment. Chambers were incubated for 3 hours, and migrating cells were counted in high-power fields (HPFs). Four measurements of MP chemotaxis were done with each protein by using same chamber at the same time. Each determination was an average of nine HPF measurements. Error bars correspond to standard deviations of the four determinations. The data shown are representative of at least three independent experiments done in this way. For TNFα production by MPs, the MPs (10^5 cells/well) were incubated with each protein (1 nM) for 14 hours, production of TNFα was studied by assaying aliquots of the culture supernatant using a TNFα enzyme-linked immunosorbent assay kit (Sigma). The error bars correspond to standard deviations of four measurements at the same conditions. The data shown are representative of at least three independent experiments done in this way. (**B**) MP production of tissue factor (white bars) and PMN release of myeloperoxidase (gray bars). MPs (10^4 cells/assay) were incubated with each protein (1 nM) for 4 hours and tissue factor activity was inferred from measurements of Factor VIIa–dependent Factor Xa formation (*5*). For measurements of myeloperoxidase activity, PMNs (3×10^6 cells/ml) were incubated with each protein (1 nM) or medium alone for 60 min, and peroxidase generation was measured based on reduction of 3,3′,5,5′-tetramethylbenzidine (*27*). Peroxidase activity is reported as percent total peroxidase activity [100% is defined as the activity observed with that number of PMNs following a 60-min exposure to phorbol ester (10 μM)]. For bothassays, the measurements and experiments were repeated, and error bars were constructed as in (A) (TNFα assay). (**C**) PMN chemotaxis. PMN migration was performed in the ChemoTX containing polycarbonate filters (5-μm pores) without PVP. Each protein (1 nM) or medium alone was added to the lower compartment, and PMNs (10^4 cells) were added to the upper compartment. Chambers were incubated for 45 min, then migrating cells were counted in HPFs. The data were obtained and analyzed as in (A) (MP chemotaxis).

bound with high affinity to cells expressing the IL-8 receptor type A (K_d = 8 nM) as did IL-8 (K_d = 1 nM) but not to those expressing type B (K_d > 200 nM). Our Scatchard analyses showed that the type A transfectants had a similar number of binding sites for human mini TyrRS as for IL-8 (*7*).

We then determined whether human TyrRS is secreted from apoptotic tumor cells as is human EMAP II. We induced apoptosis of human histiocytic lymphoma U-937 cells (*19*) by growing them in serum-free medium. Apoptosis of the treated U-937 cells was verified by a DNA fragmentation assay (*7*). Protein immunoblot analysis of the cell supernatant fraction, with a polyclonal antibody to human TyrRS (*20*), revealed that full-length TyrRS was secreted from apoptotic tumor cells, but not from cells under normal conditions (Fig. 4A). Under apoptotic conditions, the amount of secreted human full-length TyrRS increased with the incubation time (Fig. 4B). After 24 hours, more than 50% of total native human TyrRS was released from the cells (Fig. 4B). A similar proportion of mature EMAP II is secreted from U-937 cells under the same conditions (*9*).

To exclude the possibility that the apparent secretion of TyrRS was due to cell lysis, we measured the activity of cytosolic lactate dehydrogenase (LDH) in the supernatants (*21*). LDH activity in the supernatants was less than 10% of that in cell extracts and did not increase even after 72 hours of incubation (*7*). These results are consistent with the hypothesis that the increase of TyrRS in the supernatants is due to protein secretion. We also checked the permeability of the "secreting" apoptotic cells, using Trypan Blue exclusion as a test for intact cells (*22*). The apoptotic cells did not take up the stain (*7*), indicating that cell lysis was not responsible for the appearance of TyrRS in the apoptotic cell supernatant. As a further control, we investigated human alanyl-tRNA synthetase (AlaRS), which has none of the cytokine-like motifs of human TyrRS. Protein immunoblot analysis showed that, under the same apoptotic conditions, no AlaRS was secreted (*7*). Finally, we checked for activities of four other aminoacyl-tRNA synthetases in the supernatants or cell extracts of apoptotic U-937 cells. When cell extracts were used in assays with bovine tRNA, we observed aminoacylation with alanine, isoleucine, lysine, valine and, tyrosine (*7*). In contrast, when supernatants were used, only tyrosine was aminoacylated.

PMN elastase, which is released from PMNs, is a candidate protease (*23*) for cleavage of the full-length TyrRS. Addition of PMN elastase to recombinant full-length TyrRS resulted in production of a doublet of ~40-kD fragments and a ~24-kD fragment within 30 min (Fig. 5A). The ~40-kD fragments are almost the same molecular size as mini TyrRS. Sequencing of the ~40-kD fragments revealed that each has an NH_2-terminal sequence of MGDAP (*7*), as does human full-length TyrRS. Protein blot analysis revealed that the ~24-kD fragment is a COOH-terminal domain (*7*). Because this fragment is a little bigger than the COOH-terminal domain (Fig. 5A), we prepared a recombinant extended COOH-terminal domain [Pro^{344}–Ser^{528} (Fig. 5B)] to more closely reproduce the putative cleavage site recognized by PMN elastase. The extended COOH-terminal domain, which includes 17 more amino acids at the NH_2-terminus of the COOH-terminal domain (Pro^{360}–Ser^{528}), was almost the same size as the ~24-kD fragment produced by PMN elastase (Fig. 5A). We confirmed that the extended COOH-terminal domain (Pro^{344}–Ser^{528}) can induce MP and PMN chemotaxis (*7*). We also showed that recombinant truncated mini TyrRS (Met^{1}–Asp^{343}) can function as a chemoattractant for PMNs but not for MPs (*7*).

To simulate an in vivo situation, we performed two experiments. First, we added recombinant full-length TyrRS to IL-8–stimulated PMNs, which release PMN elastase (*24*). The recombinant enzyme was split into ~40-kD and ~24-kD fragments (*7*). When nonstimulated PMNs were used as a control,

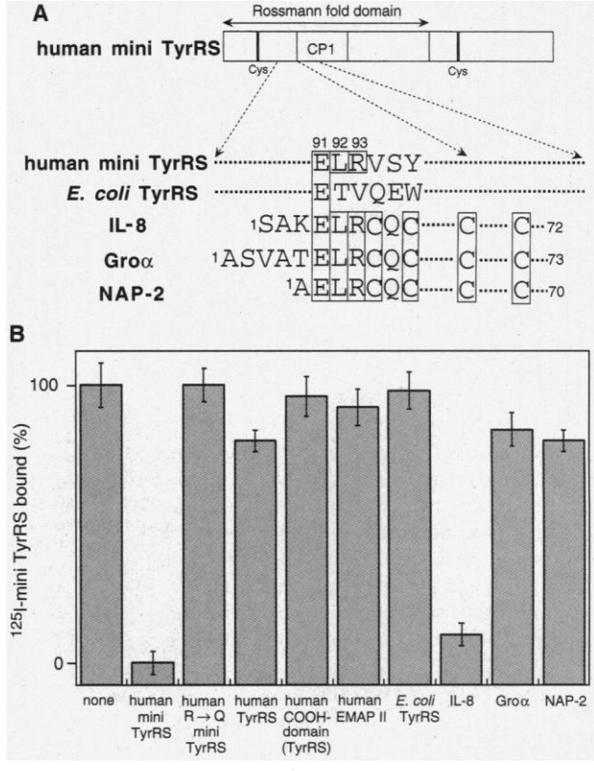

Fig. 3. Binding of "human mini TyrRS" to the PMN cellular receptor. (**A**) Schematic comparison of human mini TyrRS with other TyrRS and α-chemokines. Connective polypeptide 1 (CP1) (*28*) that splits the Rossmann nucleotide-binding fold in TyrRS is indicated. Partial alignments of native human TyrRS (*3*, *25*), *E. coli* TyrRS (*26*), mature human IL-8 (*13*), mature human Groα (*29*), and mature human NAP-2 (*30*) are shown. The ELR residues in mini human TyrRS are numbered above the sequence. Numbers on the right correspond to the terminal residues in the mature proteins (*31*). (**B**) Competition assays of ^{125}I–human mini TyrRS in the absence or presence of a 200-fold molar excess of unlabeled ligands. After incubation of PMNs with ^{125}I–human mini TyrRS (10 nM) with or without an unlabeled ligand for 2 hours, cells were separated from unbound radioactivity by centrifugation, and the cell sediment was resuspended and analyzed in a liquid scintillation counter. The maximal specific response represents 2000 counts per minute. The data represent mean values ± SD of three independent measurements.

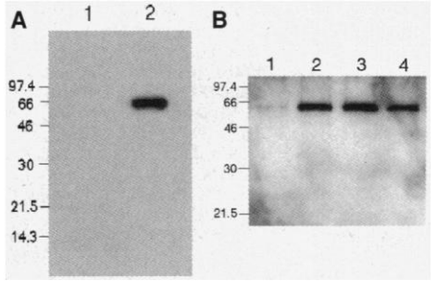

Fig. 4. Secretion of human TyrRS. Rabbit polyclonal antibodies to human TyrRS were used for protein immunoblot analysis. Samples were analyzed on 12.5% SDS-polyacrylamide gels. Molecular size markers are given to the left (in kilodaltons). (**A**) Supernatants after incubation of human U-937 cells in normal medium (lane 1) or serum-free medium (lane 2) for 24 hours. (**B**) Supernatants after incubation of the cells in a serum-free medium for 4, 12, or 24 hours (lanes 1 through 3, respectively) and the cell extract after the 24-hour incubation (lane 4). The whole supernatants were concentrated to the same volume as the whole-cell extract solution, and the same volume of samples was loaded for the protein immunoblot analysis.

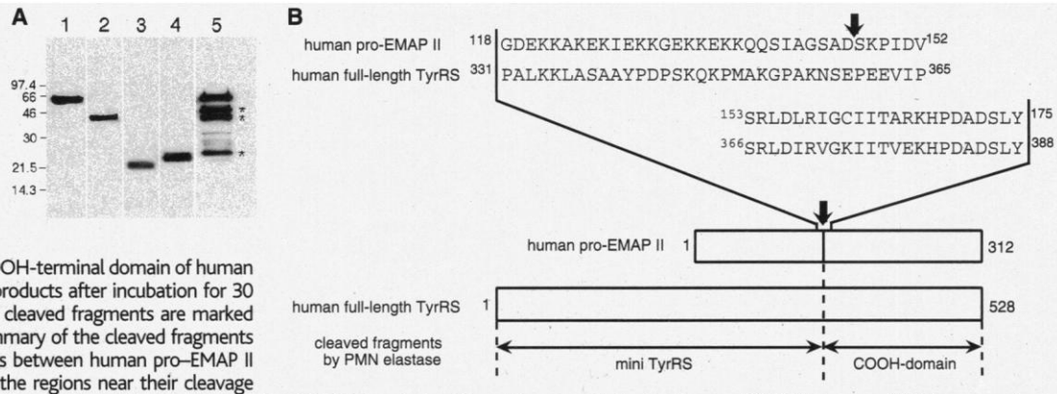

Fig. 5. Cleavage assays of human full-length TyrRS by PMN elastase. The cleavage was done in PBS (pH 7.4). A protease:protein ratio of 1:3000 was used. Immunoblot analysis was as in Fig. 4. (**A**) Protein immunoblot analyses of human full-length TyrRS (lane 1), human mini TyrRS (lane 2), COOH-terminal domain of human TyrRS (lane 3), extended COOH-terminal domain of human TyrRS (lane 4), and the cleaved products after incubation for 30 min at 37°C (lane 5). The major cleaved fragments are marked with asterisks. (**B**) Schematic summary of the cleaved fragments (*31*). Local sequence comparisons between human pro–EMAP II and human full-length TyrRS at the regions near their cleavage sites are shown on the top. Numbers at the right correspond to the COOH-terminal residues. The arrow indicates the pro–EMAP II cleavage (*5*). The approximate location of the PMN elastase cleavage site in human TyrRS is shown with a vertical dotted line.

no fragmentation of TyrRS was observed. Protein immunoblot analysis with antibodies specific for the NH_2- and COOH-terminal domain indicated that the ~40-kD and ~24-kD fragments are mini TyrRS and the COOH-terminal domain, respectively (*7*). Next, we investigated whether IL-8–stimulated PMNs would cleave the native TyrRS secreted from the apoptotic U-937 cells. In this experiment, no exogenous TyrRS was added. Incubation of IL-8–stimulated PMNs and the apoptotic cell supernatant produced the same ~40-kD and ~24-kD fragments of native TyrRS comparable to those seen in Fig. 5A (*7*).

In summary, we show that human full-length TyrRS can be split into two distinct cytokines, thus forging a link between protein synthesis and signal transduction. In principle, secretion of an essential component of the translational apparatus as an early event in apoptosis would be expected to arrest translation and thereby accelerate apoptosis. The secreted TyrRS cytokines could function as intercellular signal transducers, attracting PMNs and thus amplifying the local concentration of PMN elastase. This recursive cycle could enhance cleavage of secreted human TyrRS, thereby enhancing recruitment of macrophages to sites of apoptosis, which would promote removal of cell corpses.

References and Notes

1. M. Mirande, D. Le Corre, J.-P. Waller, *Eur. J. Biochem.* **147**, 281 (1985); M. Mirande, *Prog. Nucleic Acid Res. Mol. Biol.* **40**, 95 (1991).
2. C. Cerini *et al.*, *EMBO J.* **10**, 4267 (1991); M. Lazard and M. Mirande, *Gene* **132**, 237 (1993); K. Shiba *et al.*, *Proc. Natl. Acad. Sci. U.S.A.* **91**, 7435 (1994); S. B. Rho *et al.*, *ibid.* **93**, 10128 (1996); F. Agou and M. Mirande, *Eur. J. Biochem.* **243**, 259 (1997); S. B. Rho *et al.*, *J. Biol. Chem.* **273**, 11267 (1998).
3. T. A. Kleeman, D. Wei, K. L. Simpson, E. A. First, *J. Biol. Chem.* **272**, 14420 (1997).
4. A. I. Kornelyuk, I. V. Kurochkin, G. H. Matsuka, *Mol. Biol.* [Engl. Transl. *Mol. Biol. (Mosc.)*] **22**, 176 (1988); A. D. Wolfson, Y. A. Motorin, T. I. Ribkinska, S. F. Beresten, *J. Chromatogr.* **503**, 277 (1990).
5. Human full-length and mini TyrRSs, the extra COOH-terminal domain of human TyrRS, *E. coli* TyrRS, and human mature EMAP II (with a COOH-terminal tag of six histidine residues) were overexpressed in *E. coli* strain BL 21 (DE 3) (Novagen, Madison, WI) by induction with isopropyl β-D-thiogalactopyranoside for 4 hours. Proteins were purified on a nickel affinity column (His•Bind resin; Novagen) from the supernatant of lysed cells. Endotoxin was removed from the protein solutions by phase separation using Triton X-114 [Y. Aida and M. J. Pabst, *J. Immunol. Methods* **132**, 191 (1990); S. Liu *et al.*, *Clin. Biochem.* **30**, 455 (1997).] and was determined to be <0.01 endotoxin units per milliliter by a *Limulus* Amebocyte Lysate gel-clot assay (E-Toxate; Sigma, St. Louis, MO).
6. K. Wakasugi, C. L. Quinn, N. Tao, P. Schimmel, *EMBO J.* **17**, 297 (1998).
7. K. Wakasugi and P. Schimmel, unpublished observations. [supplementary data can be found at the *Science* Web site (www.sciencemag.org/feature/data/990263.shl)]
8. J. Kao *et al.*, *J. Biol. Chem.* **267**, 20239 (1992); J. Kao *et al.*, *ibid.* **269**, 9774 (1994); J. Kao *et al.*, *ibid.*, p. 25106.
9. M. P. R. Tas *et al.*, *Cytokine* **9**, 535 (1997).
10. Human MPs and PMNs were prepared from acid citrate dextrose–treated blood of normal healthy volunteers (*8*).
11. T. J. Daly *et al.*, *J. Biol. Chem.* **270**, 23282 (1995).
12. E. L. Becker, *Arch. Pathol. Lab. Med.* **101**, 509 (1977).
13. M. Baggiolini and I. Clark-Lewis, *FEBS Lett.* **307**, 97 (1992); R. C. Hoch, I. U. Schraufstätter, C. G. Cochrane, *J. Lab. Clin. Med.* **128**, 134 (1996); M. Baggiolini, B. Dewald, B. Moser, *Annu. Rev. Immunol.* **15**, 675 (1997).
14. C. A. Hébert, R. V. Vitangcol, J. B. Baker, *J. Biol. Chem.* **266**, 18989 (1991); I. Clark-Lewis, C. Schumacher, M. Baggiolini, B. Moser, *ibid.*, p. 23128; B. Moser *et al.*, *ibid.* **268**, 7125 (1993).
15. Custom radio-iodination of human mini TyrRS with ^{125}I was performed by Research & Diagnostic Antibody (Richmond, CA).
16. Binding assays with the radiolabeled mini TyrRS were performed as follows [B. Moser, C. Schumacher, V. von Tscharner, I. Clark-Lewis, M. Baggiolini, *J. Biol. Chem.* **266**, 10666 (1991); F. Petersen, H. D. Flad, E. Brandt, *J. Immunol.* **152**, 2467 (1994)]: PMNs (2×10^6 cells) or basophilic leukemia cells (2×10^6) in 120 μl of RPMI 1640 medium containing 20 mM Hepes (pH 7.4) and 10 mg/ml bovine serum albumin (BSA) were incubated on ice for 2 hours with 10 nM ^{125}I-human mini TyrRS (specific activity of ~60 Ci/mmol) in the absence or presence of a 200-fold molar excess of either unlabeled TyrRSs, human mature EMAP II, human recombinant IL-8 (Calbiochem, La Jolla, CA), human recombinant Groα (Biosource International, Camarillo, CA), or human recombinant NAP-2 (Biosource International). Cells were separated from unbound radioactivity by centrifugation at approximately 8000*g* for 2 min through 500 μl of a 10% sucrose/phosphate-buffered saline (PBS) cushion. The supernatant was aspirated, and the cell sediment was resuspended by using EcoLite (ICN Biomedicals, Irvine, CA) and analyzed in a scintillation counter.
17. J. Lee *et al.*, *J. Biol. Chem.* **267**, 16283 (1992).
18. I. U. Schraufstätter, M. Burger, R. C. Hoch, Z. G. Oades, H. Takamori, *Biochem. Biophys. Res. Commun.* **244**, 243 (1998).
19. L. Ghibelli, S. Coppola, C. Nosseri, A. Bergamini, S. Beninati, *FEBS Lett.* **344**, 35 (1994).
20. For the secretion assays, U-937 cells (4×10^6 cells) were cultured in RPMI 1640 medium without or with heat-treated fetal bovine serum (10%). Cells were washed twice with ice-cold PBS, and resuspended in lysis buffer containing 25 mM Hepes (pH 7.5), 5 mM EDTA, 5 mM dithiothreitol, 0.1% CHAPS detergent, 2 mM phenylmethylsulfonyl fluoride (PMSF), 10 μg/ml aprotinin, 20 μg/ml leupeptin, and 10 μg/ml pepstatin A. The cells were frozen and thawed three times in liquid nitrogen, and then centrifuged for 30 min at 4°C. For examination of proteins in the cell supernatant, 20 ml of spent culture medium (to which the following protease inhibitors were added: 2 mM PMSF, 10 μg/ml aprotinin, 20 μg/ml leupeptin, and 10 μg/ml pepstatin A) was concentrated in a Centriprep-10 (Amicon, Beverly, MA), and the samples were then analyzed on 12.5% SDS-polyacrylamide gels. After transfer onto Immobilon-P transfer membrane (Millipore, Bedford, MA), the membranes were blocked with PBS and 3% BSA, and incubated with rabbit polyclonal antibodies against human full-length TyrRS. Washed membranes were then incubated with a horseradish peroxidase–linked antibody to rabbit immunoglobulin (1:4000 dilution; Amersham Life Science, Arlington Heights, IL) for detection of TyrRS.
21. LDH activities were determined spectrophotometrically with a CytoTox 96 Non-Radioactive Cytotoxicity Assay kit (Promega, Madison, WI).
22. S. C. Wright *et al.*, *J. Cell. Biochem.* **48**, 344 (1992).
23. K. Bjørnland *et al.*, *Int. J. Oncol.* **12**, 535 (1998).
24. E. Brandt, J. Van Damme, H.-D. Flad, *Cytokine* **3**, 311 (1991).
25. L. Ribas de Pouplana, M. Frugier, C. L. Quinn, P. Schimmel, *Proc. Natl. Acad. Sci. U.S.A.* **93**, 166 (1996).
26. D. G. Barker, C. J. Burton, G. Winter, *FEBS Lett.* **150**, 419 (1982).
27. R. Menegazzi, G. Zabucchi, A. Knowles, R. Cramer, P. Patriarca, *J. Leukocyte Biol.* **52**, 619 (1992).
28. R. M. Starzyk, T. A. Webster, P. Schimmel, *Science* **237**, 1614 (1987).
29. A. Richmond *et al.*, *EMBO J.* **7**, 2025 (1988).
30. A. Walz and M. Baggiolini, *J. Exp. Med.* **171**, 449 (1990).
31. Single-letter abbreviations for the amino acid residues are as follows: A, Ala; C, Cys; D, Asp; E, Glu; F, Phe; G, Gly; H, His; I, Ile; K, Lys; L, Leu; M, Met; N, Asn; P, Pro; Q, Gln; R, Arg; S, Ser; T, Thr; V, Val; W, Trp; and Y, Tyr.

32. We thank I. U. Schraufstätter for RBL2H3 rat basophilic leukemia cells expressing IL-8 type A or B

receptor, and D. J. Loskutoff for human U-937 cells. Supported by NIH grant GM23562 and by a grant from the National Foundation for Cancer Research. K.W. was supported by a JSPS (Japan Society for the Promotion of Science) Postdoctoral Fellowships for Research Abroad.

15 January 1999; accepted 5 March 1999

ROUGH SHEATH2: A Myb Protein That Represses *knox* Homeobox Genes in Maize Lateral Organ Primordia

Marja C. P. Timmermans,[1,2] Andrew Hudson,[3] Philip W. Becraft,[4] Timothy Nelson[1]*

The regulation of members of the *knotted1*-like homeobox (*knox*) gene family is required for the normal initiation and development of lateral organs. The maize *rough sheath2* (*rs2*) gene, which encodes a Myb-domain protein, is expressed in lateral organ primordia and their initials. Mutations in the *rs2* gene permit ectopic expression of *knox* genes in leaf and floral primordia, causing a variety of developmental defects. Ectopic KNOX protein accumulation in *rs2* mutants occurs in a subset of the normal *rs2*-expressing cells. This variegated accumulation of KNOX proteins in *rs2* mutants suggests that *rs2* represses *knox* expression through epigenetic means.

Regulation of *knox* gene expression determines the emergence of lateral organs from shoot meristems. In maize, the KNOTTED-1 (KN1) homeodomain protein accumulates in cells of the shoot apex and maintains the meristematic properties of the cells (*1*). Recruitment of leaf founder cells (and the down-regulation of *kn1*) begins at a single site on the flank of the shoot apex and continues laterally around the circumference of the apex (*1, 2*). Other *knox* family members, including *rough sheath1* (*rs1*), are also implicated in leaf initiation and patterning (*3–5*).

The *knox* gene products are absent in normal leaf and floral primordia (*1, 3, 6*). Ectopic *knox* expression during organogenesis interferes with organ determination and cell differentiation along the adaxial/abaxial and proximodistal axes (*5, 7, 8*). In maize, dominant mutations in *knox* genes cause the distal displacement of sheath, auricle, and ligule tissues (*5*). In dicot species, overexpression of *knox* genes results in the development of filamentous and lobed leaves and in the formation of ectopic meristems (*8*).

[1]Department of Molecular, Cellular, and Developmental Biology, Yale University, New Haven, CT 06511, USA. [2]Cold Spring Harbor Laboratory, Post Office Box 100, Cold Spring Harbor, NY 11724, USA. [3]Institute of Cell and Molecular Biology, University of Edinburgh, Edinburgh, EH9 3JH, UK. [4]Zoology and Genetics Department, Iowa State University, Ames, IA 50011, USA.

*To whom correspondence should be addressed. E-mail: timothy.nelson@yale.edu

In maize, recessive mutations that affect *knox* gene repression have also been identified. The *narrow sheath* and *leafbladeless1* mutations affect *kn1* down-regulation at leaf initiation, resulting in deletion of the leaf margins and development of radially symmetrical, abaxialized leaves, respectively (*9*). Mutations in *rs2* result in proximodistal patterning defects that are due to *rs1* and *kn1* expression in leaf primordia (*10*). Recessive mutations in the *PHANTASTICA* (*PHAN*) gene of *Antirrhinum*, which encodes a Myb-domain protein, exhibit phenotypes that resemble the phenotypes of these maize mutants (*6, 11*). Therefore, we investigated the *phan* homolog from maize (*12*).

The maize *phan* homolog encodes a 370–amino acid protein with a 106–amino acid NH_2-terminal Myb domain consisting of two Myb-like repeats (Fig. 1A). The Myb domain and COOH-terminus share a high degree of amino acid identity with PHAN proteins from *Antirrhinum* and *Arabidopsis*. The DNA recognition helices of PHAN share little homology with the other large class of plant Myb proteins (*13*), suggesting that the PHAN proteins regulate a different class of target genes. However, the PHAN proteins do not contain motifs that suggest a direct transcriptional function. A single intron in the 5′ untranslated region (UTR), ~50 nucleotides upstream of the translation initiation codon, indicates a structural relation between the *Antirrhinum* and maize *phan* genes (Fig. 1B) (*12*).

The maize *phan* homolog was mapped to a region on chromosome arm 1S that contains a potential *knox* gene regulator, the *rs2* gene (*14*). A comparison of the structure of the *phan* locus in wild type and in three mutant alleles of *rs2* confirmed that *rs2* is the maize homolog of *phan* (Fig. 1B) (*15*). The *rs2* mutations cause leaf and floral phenotypic alterations analogous to the phenotypes induced by mutations that alter the regulation of *knox* genes during lateral organ initiation or development (*5, 10*).

We compared the pattern of KNOX protein expression in wild-type and *rs2* mutant apices by immunolocalization with an antibody specific to KNOX proteins, including KN1 and RS1 (*10, 16*). KNOX proteins accumulated in the shoot apex and stem of wild-type plants but were absent at leaf initiation sites on the apex and in leaf primordia (*1*) (Fig. 2, A and C). In *rs2* mutants, KNOX proteins accumulated normally in the meristem and stem, but they also accumulated at the base of leaf primordia and near major lateral veins in the leaf (Fig. 2, B and D). The ectopic accumulation of KNOX protein in patches with sharp lateral boundaries suggests that the leaves were clonal mosaics of *knox*+ and *knox*– sectors (Fig. 2B). Sectors expressing KNOX proteins varied among leaves and did not correlate with normal developmental domains. The down-regulation of *knox* expression at the initial site of founder cell recruitment near the center of the new leaf occurred normally in *rs2* mutants (Fig. 2D), although the number of founder cells that were recruited laterally was variably reduced.

These patterns of KNOX protein accumulation were compared to the distribution of *rs2* and *kn1* transcripts (*17*). In wild-type apices, *rs2* transcripts accumulated throughout the P1 leaf primordium, but in later stages of leaf development (P2 through P5), *rs2* expression became more restricted to the major vascular bundles and leaf margins (Fig. 3A). *rs2* was not expressed in the meristem, but expression was observed late during founder cell recruitment, at the transition from the P0 to the P1 stage. In contrast, *kn1* was expressed in meristematic cells of the shoot apex but was absent in early leaf founder cells (early P0 stage) (Fig. 3B). No *rs2* transcripts were detected in the reference allele of *rs2* (*rs2-R*) mutant shoot apices (Fig. 3C), but the *kn1* expression pattern in the meristem was unaltered. As in vegetative apices, *kn1* expression was limited to meristematic cells in flowers and was down-regulated in floral organ primordia and their initials (Fig. 3, E and H). *rs2* transcripts accumulated relatively early in founder cells of floral organ primordia (Fig. 3, D and G), and *rs2* expression per-